J. Radiat. Res., 52, 789–796 (2011)

Preliminary Calculation of RBE-weighted Dose Distribution for Cerebral Radionecrosis in Carbon-ion Treatment Planning

Yuki KASE[1*†], Takeshi HIMUKAI[1], Ai NAGANO[1], Yuji TAMESHIGE[2], Shinichi MINOHARA[1], Naruhiro MATSUFUJI[1], Junetsu MIZOE[3], Piero FOSSATI[3,4], Azusa HASEGAWA[1] and Tatsuaki KANAI[5]

Carbon-ion radiotherapy/Cerebral radionecrosis/RBE-weighted dose/Microdosimetry.

Cerebral radionecrosis is a significant side effect in radiotherapy for brain cancer. The purpose of this study is to calculate the relative biological effectiveness (RBE) of carbon-ion beams on brain cells and to show RBE-weighted dose distributions for cerebral radionecrosis speculation in a carbon-ion treatment planning system. The RBE value of the radionecrosis for the carbon-ion beam is calculated by the modified microdosimetric kinetic model on the assumption of a typical clinical α/β ratio of 2 Gy for cerebral radionecrosis in X-rays. This calculation method for the RBE-weighted dose is built into the treatment planning system for the carbon-ion radiotherapy. The RBE-weighted dose distributions are calculated on computed tomography (CT) images of four patients who had been treated by carbon-ion radiotherapy for astrocytoma (WHO grade 2) and who suffered from necrosis around the target areas. The necrotic areas were detected by brain scans via magnetic resonance imaging (MRI) after the treatment irradiation. The detected necrotic areas are easily found near high RBE-weighted dose regions. The visual comparison between the RBE-weighted dose distribution and the necrosis region indicates that the RBE-weighted dose distribution will be helpful information for the prediction of radionecrosis areas after carbon-ion radiotherapy.

INTRODUCTION

Charged particle beams are very suitable for the treatment of deeply seated cancer due to their excellent dose distribution, referred to as the Bragg peak, in the body. Furthermore, heavy-ion beams with high LET characteristics possess high relative biological effectiveness (RBE). From the years 1977 to 1993, helium-, carbon-, neon-, silicon-, and argon-ion beams were applied as heavy-ion radiotherapy at the Lawrence Berkeley National Laboratory in the United States.[1)] In 1994, routine carbon-ion radiotherapy was started using the Heavy Ion Medical Accelerator in Chiba (HIMAC) at the National Institute of Radiological Sciences (NIRS) in Japan.[2)] Presently, carbon-ion radiotherapy has also been carried out at the Hyogo Ion Beam Medical Center,[3)] the Heidelberg Ion Therapy Center,[4)] the Gunma University Heavy Ion Medical Center and so on.[5)]

For carbon-ion radiotherapy, it is essential to calculate not only the absorbed dose but also the RBE value at any point in patient's body, as the RBE values vary greatly depending on the depth within the material. In the treatment planning system (TPS), the RBE values are currently calculated on the basis of the cell survival of typical tumor cells.[6,7)] However, it is well known that the RBE value depends on the tissue type and specific biological endpoint induced by radiation. Thus, each RBE value should be essentially calculated to estimate the intended biological effect.

The purpose of this study is to establish an estimation technique of radiation damage using the physical beam calculation with an RBE calculation model for carbon-ion radiotherapy. In this paper, we reported RBE-weighted dose

*Corresponding author: Phone: +81-55-989-5222,
Fax: +81-55-989-5634,
E-mail: y.kase@scchr.jp

[1]Research Center for Charged Particle Therapy, National Institute of Radiological Sciences, 4-9-1 Anagawa, Inage-ku, Chiba-shi, Chiba 263-8555, Japan; [2]Proton Therapy Center, Fukui Prefectural Hospital, 2-8-1 Yotsui, Fukui-shi, Fukui 910-8526, Japan; [3]CNAO Foundation, National Center for Oncological Hadrontherapy, Via Caminadella, Milano, Italy; [4]University of Milan, Biomedical Sciences and Technologies Department, Via Festa del Perdono, Milano, Italy; [5]Heavy Ion Medical Center, Gunma University, 3-39-22, Showa, Maebashi-shi, Gunma 371-8511, Japan.

[†]Currently working at Proton Therapy Division, Shizuoka Cancer Center Research Institute, 1007, Shimonagakubo, Nagaizumi-cho, Shizuoka 411-8777, Japan.

doi:10.1269/jrr.11044

distributions calculated on trial to estimate position of cerebral radionecrosis induced by carbon-ion beams. The location information of radionecrosis is detectable with magnetic resonance imaging (MRI) brain scans[8] and is important for the patient's prognosis after radiotherapy.[9,10] At the NIRS, astrocytomas have been treated with carbon-ion beams since 1994, and the dose escalation study is in progress.[2,11] In this study, four patients with the astrocytoma (WHO grade 2) treated with carbon-ion beams were selected to demonstrate the visual comparison between the RBE-weighted dose distribution and detected necrosis region.

The microdosimetric kinetic model (MKM)[12] modified for range-modulated ion beams was used to account for the physical dependence of the RBE value on the carbon-ion irradiation field.[13] Inaniwa *et al.* has applied the modified MKM to the treatment planning system for scanned carbon-ion beams.[14] The RBE value in the bodies of patients was calculated from microdosimetric quantities measured by a tissue-equivalent proportional counter (TEPC) for monoenergetic carbon-ion beams. In addition, the clinical α/β ratio described in the literature for X-ray radiotherapy was used to consider the tissue dependence of the RBE value for the heavy-ions.

MATERIALS AND METHODS

RBE calculation model

For carbon-ion radiotherapy in Japan, the Bragg peak is spread out by modulating the beam range to sterilize tumor cells uniformly throughout the tumor volume. The therapeutic carbon-ion beams were designed to effect a 10% survival fraction for the HSG cells in the region of the spread-out Bragg peak (SOBP).[15] However, even if the survival fraction of the HSG cells is constant in the SOBP, it may be inhomogeneous for other cell lines, tissues, endpoints, or circumstances because the RBE value typically depends on the biological conditions. In this study, the RBE value for cerebral radionecrosis was calculated by the modified MKM with the clinical data of α/β ratios for X-rays.

In the modified MKM, the surviving fraction, S, of certain cells is calculated with the biological model parameters (α_0, β, r_d, and y_0), as follows:[13]

$$S = \exp\left[-\alpha D - \beta D^2\right], \tag{1}$$

$$\alpha = \alpha_0 + \frac{\beta}{\rho\pi {r_d}^2} y^*, \tag{2}$$

$$y^* = \frac{{y_0}^2 \int \left(1 - \exp(-y^2 / {y_0}^2)\right) f(y) dy}{\int y f(y) dy}, \tag{3}$$

where ρ is the density of tissue assumed to be ρ = 1 g/cm^3, f(y) is the probability density of the lineal energy, y, and y^* is the saturation-corrected dose-mean lineal energy.

The biological model parameters except for the α_0 value was assumed to be the same as those obtained for HSG cells (β = 0.05 Gy^{-2}, r_d = 0.42 μm, and y_0 = 150 keV/μm).[13] The α_0 value was assumed to be the only parameter dependent on tissue or the clinical endpoint, and it was fitted with reference to the clinical α/β ratio for X-rays because the biological parameters in a clinical situation was presently limited to α/β ratios obtained by many fractionation studies in conventional X-ray radiotherapy. Clinical α/β ratios have been reported, for example, α/β = 2 Gy for cerebral radionecrosis and α/β = 10 Gy for a typical early effect for X-rays.[16] In order to have equalities of α/β = 2 Gy and α/β = 10 Gy for X-rays, the α_0 values were calculated to be 0.04 and 0.44 Gy^{-1}, respectively. Figure 1 shows the y^*-α curve obtained for the *in-vitro* HSG cells and the y^*-α curves estimated by the modified MKM in assuming the α/β ratios from 1 to 10 Gy.

When the absorbed dose and the α value with the fixed β value are determined, the RBE value is calculated as follows:

$$RBE = \frac{D_R}{D} = \frac{\sqrt{{\alpha_R}^2 + 4\beta\left(\alpha D + \beta D^2\right)} - \alpha_R}{2\beta D}, \tag{4}$$

where D is the absorbed dose for the radiation of interest and D_R is the absorbed dose at the same survival fraction for a reference radiation which is X-rays of 200 kVp in this study. The RBE-weighted dose, D_{RBE}, is defined as follows:

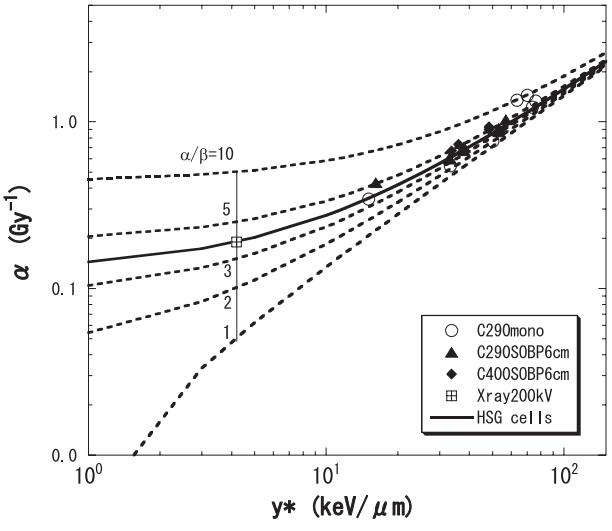

Fig. 1. The α values as a function of the microdosimetric y^* value with β = 0.05 Gy^{-2} fixed. The plots show the experimental data obtained by the *in-vitro* HSG cells and the y^* value measured by the TEPC.[12] The solid curve shows the modified MKM calculations for the *in vitro* HSG cells. Dashed curves show the model estimation assuming α/β ratios from 1 to 10 for X-rays.

$$D_{RBE} = RBE \cdot D = \frac{\sqrt{\alpha_R{}^2 + 4\beta\left(\alpha D + \beta D^2\right)} - \alpha_R}{2\beta}, \qquad (5)$$

where the unit of Gy(RBE) in this paper is used for the D_{RBE} value when the unit of Gy is used for the D value.

Microdosimetric y* *measurement*

The microdosimetric y^* value is necessary to calculate the RBE value using the modified MKM, as described in the previous chapter. The y^* distributions were measured using the TEPC (LET-1/2; Far West Technology, Inc.) in order to estimate the RBE value for therapeutic carbon-ion beams.[16] The sensitive volume of the counter was nominally a sphere of 12.7-mm diameter, around which a spherical wall of A-150 tissue-equivalent plastic (thickness: 1.27 mm) was situated. The wall was housed in an aluminum shell (thickness: 0.178 mm) to maintain a proportional gas under low pressure. The propane-based tissue-equivalent gas (p-TEG; 54.6% C_3H_8, 40.16% CO_2, and 5.26% N_2, by volume) was enclosed with a pressure of 4.4 kPa in the counter to simulate the energy imparted to a spherical tissue with a unit density of 1.0-μm diameter. The TEPC was operated with a voltage bias of + 640 V. The electric impulse from the counter entered a pre-amplifier (preamplifier 142B; ORTEC), and the pre-amplified output signal was then divided to enter three linear amplifiers of 2, 30, and 450 gains (amplifier 572/671; ORTEC) to realize a wide measurement range and fine energy resolution. These signals were stored in multichannel analyzers (MCA8000A; AMPTEK). A calibration pulser was used to examine the linearity between the pulse height of the preamplifier output and the channel and to relate those channels of the three spectra.

Calculation of RBE-weighted dose for therapeutic carbon-ion beams

The microdosimetric y^* distributions of therapeutic carbon-ion beams were calculated from those measured by the TEPC for the mono-energetic carbon-ion beam in each initial beam energy because measuring those for all therapeutic carbon-ion beams was difficult to achieve with a limited beam time. Figure 2 shows the depth-dose distributions measured by the Markus ionization chamber for mono-energetic carbon-ion beams with initial energies of 290, 350, and 400 MeV/u. Figure 3 shows the depth-y^* distributions measured by the TEPC for mono-energetic carbon-ion beams with initial energies of 290, 350, and 400 MeV/u.

The absorbed dose, D_m, and y^* value, y^*_m, of the range-modulated beam are calculated from those of the mono-energetic beams, as follows:

$$D_m(x) = \sum_i d_i(x + s_i) r_i, \qquad (6)$$

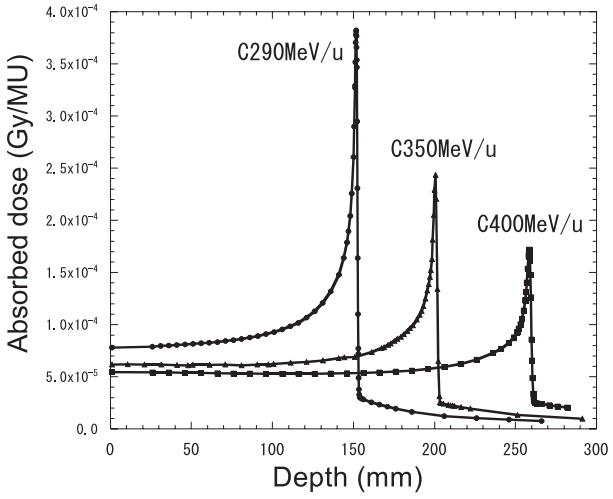

Fig. 2. Depth-dose distributions measured by the parallel-plate ionization chamber for mono-energetic carbon-ion beams with initial energies of 290, 350, and 400 MeV/u.

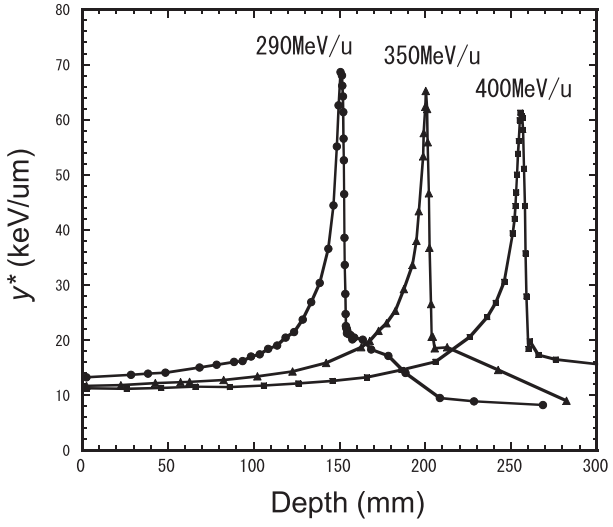

Fig. 3. Depth-y^* distributions measured by the TEPC for mono-energetic carbon-ion beams with initial energies of 290, 350, and 400 MeV/u.

$$y^*_m(x) = \frac{\sum_i y^*(x + s_i) d_i(x + s_i) r_i}{\sum_i d_i(x + s_i) r_i}, \qquad (7)$$

where $d_i(x)$ and $y^*(x)$ are absorbed dose and y^* value, respectively, at a depth of x in the mono-energetic beam, r_i is the weighting factor required for the superimposition with the shifted depth of s_i. The survival fraction and the RBE-weighted dose in the range-modulated carbon-ion beam were calculated from the absorbed dose and y^* value in the modulated beams by Eqs. (1)–(5).

RBE-weighted dose distribution on CT images

The treatment planning system, XiO-carbon combined with FocalPro (CMS Inc., St. Louis, MO), was used to calculate the RBE-weighted dose distribution on the CT image. In order to apply the effective SOBP dose calculation for carbon-ion TPS, the alternative effective percent depth dose (PDD) for superposition was determined by adjusting the range offset and weight.[18] The effective PDD was obtained by multiplying the absorbed dose distribution by the RBE value at the survival fraction of central SOBP depth to reproduce the RBE-weighted dose distribution calculated by the modified MKM for the cerebral radionecrosis.

In this study, we selected four patients who had astrocytoma (WHO grade 2) treated by carbon-ion beams and suffered from cerebral radionecrosis around the planning target volume (PTV). The patients were diagnosed with astrocytoma (WHO grade 2) by biopsy, surgery to remove part of the tumor, or postoperative recurrence. Before carbon-ion radiotherapy, these patients gave written informed consent, accepting the possibility that radionecrosis might occur as a result of the treatment, and the institutional ethics committee approved the study. CT images of the patients were used to calculate the RBE-weighted dose distributions for radionecrosis in the TPS. The PTVs in these patients were irradiated with the clinical dose of 50.4 GyE in 24 fractions (2.1 GyE/fraction) at the target reference point from two beam directions. Table 1 summarizes the therapeutic beam conditions of the patients.

In the case of carbon-ion treatment of brain tumor at NIRS, contrast-enhanced MRI has been typically performed to check for irradiation effect once in the middle of the treatment, once within a week after the treatment, every month for half year, and every few months for next half year. Afterward, prolonged observation with the MRI and other diagnostic imaging such as ^{11}C-methionine positron emission tomography (MET-PET) were performed every month from one or two years after the carbon-ion treatment in order to diagnose tumor recurrence, cerebritis, necrosis and so on for follow-up care. The astrocytoma (WHO grade 2) is not commonly enhanced by the MRI. However, in rare cases, it was partially faintly-enhanced or was diagnosed with malignant change by further surgery when new enhanced area appeared during follow-up after the irradiation and surgery. Detailed clinical results of carbon-ion radiotherapy for astrocytomas (WHO grade 2) have been reported by Hasegawa *et al.*[19]

The axial contrast-enhanced T1-weighted MRI brain images obtained at 7–12 months after the carbon-ion radiotherapy were used to draw the contours of radionecrosis regions in this study. The contrast area of the MRI was suspected to be the necrosis region, which could internally include some non-contrast regions. However, some of the necrosis regions might be tumor necrosis though they basically had been non-tumor volume until the carbon irradiation and included in the irradiation area. The necrosis regions were contoured in view of signal intensity, post contrast enhancement and evolution in subsequent exams. All the contoured regions were fused with the CT images, based on anatomic landmark such as eyeballs, ventricular systems, frontal poles of temporal lobes and fissures.

RESULTS

RBE-weighted dose calculated from TEPC measurement

Figure 4 shows the survival fractions calculated by the modified MKM for cerebral radionecrosis as a function of depth for the 290 MeV/u carbon-ion beam with 6-cm SOBP width when the prescribed dose was 2.1 GyE in the clinical dose or 0.87 Gy in absorbed dose at the center of the SOBP region. The calculated results with α/β values of 1, 2, 5, 10 Gy for X-rays are shown to represent the dependence of the survival distribution on the α/β value with the β value fixed to 0.05 Gy^{-2}. The symbols in Fig. 4 show the results calculated using the y^* values measured by the TEPC for the range-modulated carbon-ion beam in the case of an α/β ratio of 2 Gy for X-rays. It was confirmed that the measured mono-energetic depth-y^* distribution was available to reproduce the survival distribution calculated from the TEPC measurement for the range-modulated carbon-ion beam. The survival fraction with an α/β ratio of 2 Gy for X-rays was calculated to be 0.62 at the proximal SOBP and 0.58 at the distal SOBP for the 290 MeV/u carbon-ion beam with 6-cm SOBP width when the prescribed dose was 2.1 GyE in the clinical dose. Thus, the biological effect is inclined to increase with the depth in the SOBP region in the case of the low α/β ratio around 2 Gy, while it tends to decrease in

Table 1. Beam conditions applied for four patients in carbon-ion radiotherapy

Patient		Beam 1				Beam 2			
No.	PTV (cc)	Energy (MeV/u)	SOBP (cm)	Range (cm)	Air gap (cm)	Energy (MeV/u)	SOBP (cm)	Range (cm)	Air gap (cm)
1	64.9	290	8	13.9	13.84	290	6	8.5	9.20
2	106.7	290	10	9.43	16.22	290	8	8.38	11.72
3	59.3	290	7	11.8	16.61	290	7	12.61	16.46
4	141.2	350	8	16.66	9.49	290	8	8.54	10.34

the case of the high α/β ratio around 10 Gy, at the clinical dose level of 2.1 GyE. The depth-survival distribution in the SOBP region was found to be roughly constant around the α/β ratio of 5 Gy for X-rays among these distributions, since the ridge filter was designed for the HSG cells close to that α/β ratio. This result shows the tissue-type dependence of the RBE value for carbon-ion beam can be calculated from the α/β values for X-rays.

Figure 5 shows the RBE-weighted dose distributions for the 290 MeV/u carbon-ion beams with SOBP widths from 2 to 12 cm when the prescribed dose was 2.1 GyE in the clinical dose. Note that the RBE-weighted dose is different from the clinical dose even under the same physical beam condition because of the difference of RBE value between the cerebral necrosis and tumor cell killing. Thus, the RBE-weighted dose for cerebral necrosis became inhomogeneous in spite of the uniform clinical dose in the SOBP region. The calculated RBE-weighted dose provided good agreement with that derived from the y^* values measured by the TEPC for the 290 MeV/u carbon-ion beam with the 6-cm SOBP width. The difference between the proximal and distal peaks was 11% for the 12-cm SOBP width at this dose level. Therefore, the incidence rate of the cerebral radionecrosis is thought to be larger as the depth is closer to the distal peak in the SOBP region.

RBE-weighted dose calculated in the TPS

Figure 6 shows the absorbed dose and RBE-weighted dose distributions calculated for the therapeutic carbon-ion beams with the SOBP width of 6 cm and the initial energies of 290, 350 and 400 MeV/u when the prescribed dose was 2.1 GyE in the clinical dose. The RBE-weighted dose

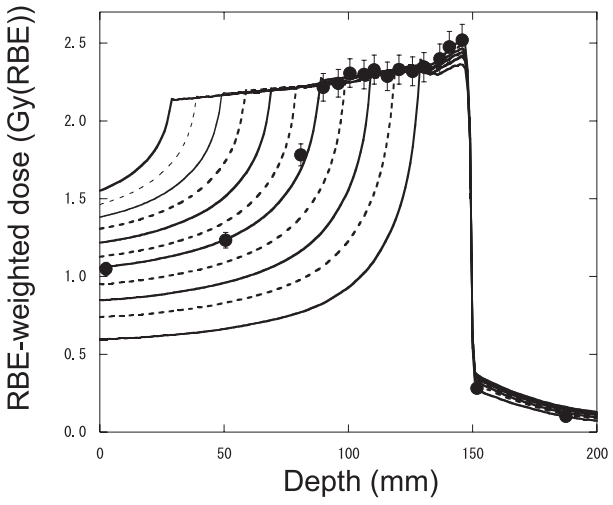

Fig. 5. RBE-weighted dose distributions calculated for cerebral radionecrosis in the 290 MeV/u carbon-ion beams with the SOBP width from 2 to 12 cm when the prescribed dose was 2.1 GyE in the clinical dose. The symbols were calculated from the y^* values measured by the TEPC for the 290 MeV/u carbon-ion beam with the 6-cm SOBP.

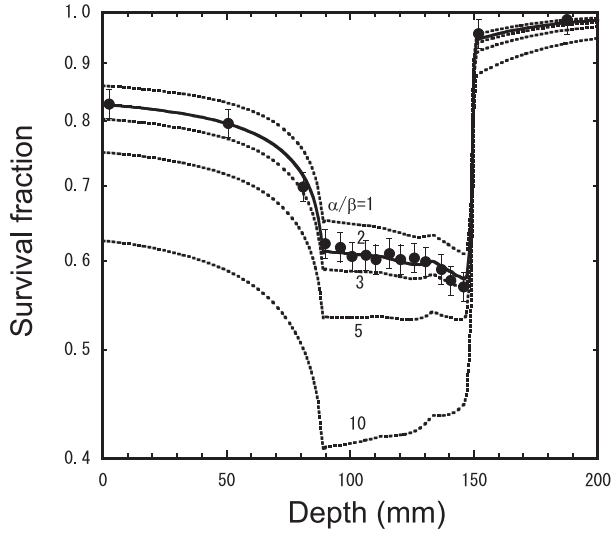

Fig. 4. Survival fractions at different depths for the 290 MeV/u carbon-ion beam with 6-cm SOBP when the prescribed dose was 2.1 GyE in the clinical dose or 0.87 Gy in the absorbed dose at the center of the SOBP. Circles were calculated by the modified MKM from the y^* values measured by the TEPC, assuming that α/β = 2 Gy for X-rays. Lines show the calculated curves using the y^* and absorbed dose measured with the mono-energetic 290 MeV carbon-ion beam in assuming the α/β ratios from 1 to 10 Gy.

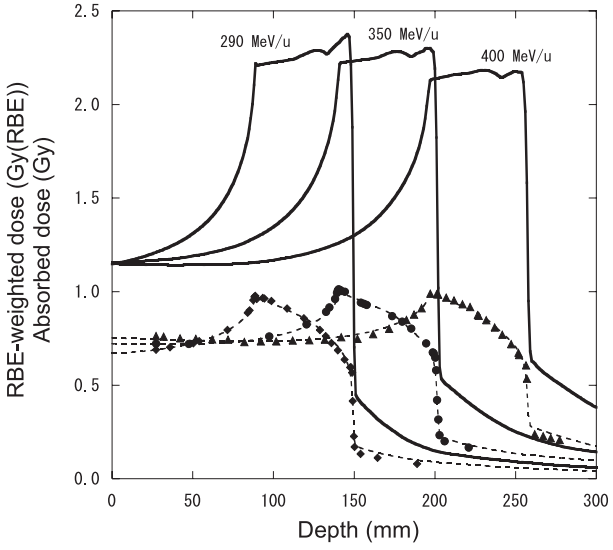

Fig. 6. Absorbed dose and RBE-weighted dose distributions with 6-cm SOBP width for 290, 350 and 400 MeV/u carbon-ion beams when the prescribed dose is 2.1 GyE in the clinical dose. Dashed lines were calculated from the mono-energetic distribution measured by the ionization chamber. Plots show the ionization chamber measurement for the therapeutic SOBP beams. Solid lines were calculated by the modified MKM in assuming that α/β = 2 Gy for X-rays.

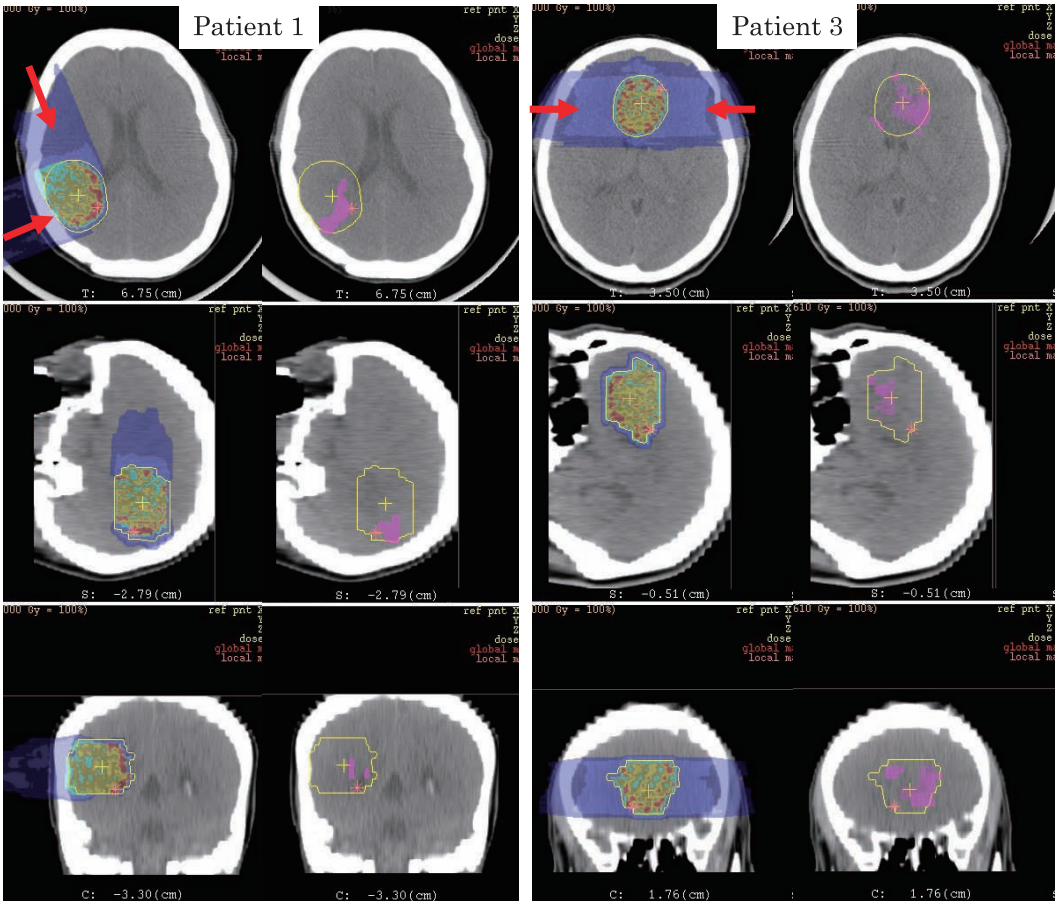

Fig. 7. Comparisons between the RBE-weighted dose distributions (left) and the necrotic regions (right). The yellow contours and cross marks represent the PTV and the reference point used to give the prescribed dose, respectively. Isodose levels show 103% (red), 102% (orange), 101% (yellow), 100% (dark yellow), 90% (cyan), 50% (blue), and 30% (dark blue) of 56.0 Gy(RBE) in the RBE-weighted dose. Red arrows indicate the therapeutic beam directions.

around the distal SOBP region was found to decrease with incident beam energy because the percentage of fragment particles with low RBE increases with the penetration depth. In this dose level, the RBE-weighted dose gradient in the SOBP region for the 350 MeV/u was smaller than that for the 290 MeV/u.

Figure 7 shows visual comparisons between the RBE-weighted dose distribution and the detected necrosis region on the CT images for patients 1 and 3. The 100% level of the isodose line was set to be the RBE-weighted dose of 56.0 Gy(RBE) at the reference point of patient 1. The same isodose level was also used for patients 3 in order to measure these distributions with the same absolute RBE-weighted dose scale. The global maximum RBE-weighted doses were 60.5, 59.9, 60.3 and 58.1 Gy(RBE) for patients 1, 2, 3 and 4, respectively. The difference of the dose distribution among the patients was caused by beam conditions such as the beam energy, the irradiation angle, the range shifter thickness and the SOBP width, and geometrical conditions such as the air gap between beam delivery snout and skin, and the thickness of skull bone. In the case of patient 1, the necrotic volumes were found near high RBE-weighted dose region around rear part of SOBP region. In the case of patient 3, the high RBE-weighted dose regions were found throughout the PTV, and the necrotic areas were also detected in whole PTV. These results indicate that the RBE-weighted dose distribution will be effective for location estimation of cerebral radionecrosis by considering the dependence of the RBE value on tissue type and dose level in the TPS.

DISCUSSION

Assumptive fixed β value

The assumptive β value of 0.05 Gy^{-2} for the cerebral radionecrosis is thought to be reasonable as an average β value of human brain cells in reference to the presented β values of the *in vitro* brain cells ranging from 0.02 to 0.1 Gy^{-2} for X-rays.[20] However, it was realistically quite difficult to evaluate the appropriateness for the actual *in vivo* β values of human brain cells. The absolute survival fraction depends

on the β value, so the calculated survival fraction may be different from the actual survival fraction in the human brain. The RBE-weighted dose in Eq. (5) is transformed with Eq. (2), as shown in the following equation,

$$D_{RBE} = \sqrt{\frac{1}{4}\left(\frac{\alpha_R}{\beta}\right)^2 + D^2 + \left(\frac{\alpha_0}{\beta} + \frac{y^*}{\rho\pi r_d^{\,2}}\right)D} - \frac{1}{2}\left(\frac{\alpha_R}{\beta}\right). \quad (8)$$

If the α_R/β, α_0/β, and y^*/r_d^2 ratios are constant, the RBE-weighted dose remains unchanged by the β value. Therefore, we think that the α/β ratios are more important to determine the RBE-weighted dose distribution than the β value in the MKM calculation.

Difference between the RBE-weighted dose distribution and the detected necrotic region

The geometric differences between the RBE-weighted dose distributions and the detected necrosis regions are thought to have many causes: 1) patient positioning errors; 2) postural changes in the patient among the CT scans, treatment irradiation, and MRI scans; 3) image fusion error between the CT and MR images; 4) shape changes of the tumor and surrounding tissues; 5) inhomogeneous radiosensitivity or brain structure; 6) transformation of the necrotic region; 7) errors in the RBE model and model parameters; 8) TPS calculation error; 9) the fundamental difference between single cell survival and complex tissue effects. At this time, a practical solution to these problems would be very difficult because there are not enough case reports regarding cerebral radionecrosis after carbon-ion radiotherapy.

In terms of the inhomogeneous radiosensitivity, a higher risk of brain necrosis in the subependymal area has been reported[21] and has also been observed in the small population of patients with low-grade astrocytoma treated with carbon-ion radiotherapy at NIRS. As for the transformation of necrotic regions, brain necrosis is specially self-sustained and tends to expand; as such, the necrotic voxel observed some months after radiotherapy may not be directly induced by the radiation because the necrotic area has transformed, including the original necrotic area.

In terms of the difference between cell survival and tissue effect, we assumed that cell survival was only a local phenomenon, meaning that dose in one voxel should predict survival in that voxel, disregarding any bystander effect. On the contrary, brain necrosis risk in one voxel may be dependent not only on dose in that voxel but also on dose in the voxels nearby. Figure 8 shows the probabilities of the cerebral necrosis with respect to each voxel as a function of the RBE-weighted dose calculated in the TPS for the four patients. It was found that the necrosis probability tended to increase with the RBE-weighted dose. However, there was great variability of the probability curve among the patients. The general model for normal tissue complication probability was not adequate to estimate the punctual risk of brain necrosis according the RBE-weighted dose distribution. Thus more elaborate analysis with the RBE-weighted dose must be carried out to estimate the macroscopic necrosis risk, considering the various types of geometrical and calculation uncertainties.

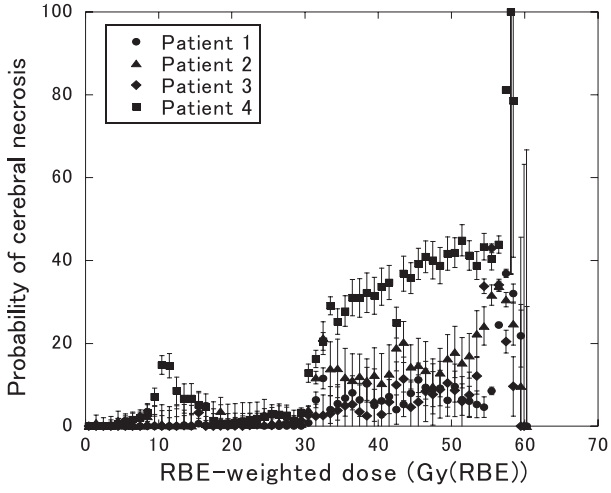

Fig. 8. Probabilities of the cerebral necrosis with respect to each voxel within the brain as a function of the RBE-weighted dose calculated in the treatment planning system for the four patients.

ACKNOWLEDGMENTS

The authors are grateful to Drs. Nobuyuki Kanematsu, Manabu Mizota, Naoaki Kondo and Hiroshi Asakura for their help in using the XiO-carbon software. This study was performed as a part of the Research Project with Heavy Ions at NIRS-HIMAC.

REFERENCES

1. Tobias CA, Wenke RP and Benton EV (1973) Heavy-particle radiotherapy. Science **182**: 474–476.
2. Tsujii H, *et al* (2007) Clinical results of carbon ion radiotherapy at NIRS. J Radiat Res **48**: A1–A13.
3. Demizu Y, *et al* (2009) Analysis of vision loss caused by radiation-induced optic neuropathy after particle therapy for head-and-neck and skull-base tumors adjacent to optic nerves. Int J Radiat Oncol Biol Phys **75**: 1487–1492.
4. Combs SE, *et al* (2010) Heidelberg Ion Therapy Center (HIT): Initial clinical experience in the first 80 patients. Acta Oncologica **49**: 1132–1140.
5. Kitagawa A, *et al* (2010) Review on heavy ion radiotherapy facilities and related ion sources. Rev Sci Instrum **81**: 02B909.
6. Endo M, *et al* (1996) HIPLAN- a heavy ion treatment planning system at HIMAC. J Japan Soc Ther Radiol Oncol **8**: 231–238.
7. Krämer M and Scholz M (2000) Treatment planning for heavy-ion radiotherapy: calculation and optimization of biologically effective dose. Phys Med Biol **45**: 3319–3330.

8. Kishimoto R, *et al* (2005) MR imaging of brain injury induced by carbon ion radiotherapy for head and neck tumors. Magnetic Resonance in Medical Sciences **4**: 159–164.
9. Ruben JD, *et al* (2006) Cerebral radiation necrosis: incidence, outcomes, and risk factors with emphasis on radiation parameters and chemotherapy. Int J Radiat Oncol Biol Phys **65**: 449–508.
10. Miyawaki D, *et al* (2009) Brain injury after proton therapy or carbon ion therapy for head-and-neck cancer and skull base tumors. Int J Radiat Oncol Biol Phys **75**: 378–384.
11. Mizoe J, *et al* (2007) Phase I/II clinical trial of carbon ion radiotherapy for malignant gliomas: combined X-ray radiotherapy, chemotherapy, and carbon ion radiotherapy. Int J Radiat Oncol Biol Phys **69**: 390–396.
12. Hawkins R-B (2003) A microdosimetric-kinetic model for the effect of non-Poisson distribution of lethal lesions on the variation of RBE with LET. Radiat Res **160**: 61–69.
13. Kase Y, *et al* (2006) Microdosimetric measurements and estimation of human cell survival for heavy-ion beams. Radiat Res **166**: 629–638.
14. Inaniwa T, *et al* (2010) Treatment planning for a scanned carbon beam with a modified microdosimetric kinetic model. Phys Med Biol **55**: 6721–6737.
15. Kanai T, *et al* (1999) Biophysical characteristics of HIMAC clinical irradiation system for heavy-ion radiation therapy. Int J Radiat Oncol Biol Phys **44**: 201–210.
16. Steel GG (2000) Basic clinical radiobiology. Arnold (London): a member of the Hodder Headline Grroup.
17. Kase Y, *et al* (2011) Microdosimetric approach to NIRS-defined biological dose measurement for carbon-ion treatment beam. J Radiat Res **52**: 59–68.
18. Koyama-Ito H, *et al* (2007) Carbon-ion therapy for ocular melanoma: planning orthogonal two-port treatment. Phys Med Biol **52**: 5341–5352.
19. Hasegawa A, *et al* (2011) Experience of carbon ion radiotherapy for diffuse astrocytomas (WHO grade 2). Int J Radiat Oncol Biol Phys, accepted for publication.
20. Suzuki M, *et al* (2000) Relative biological effectiveness for cell-killing effect on various human cell lines irradiated with heavy-ion medical accelerator in Chiba (HIMAC) carbon-ion beams. Int J Radiat Oncol Biol Phys **48**: 241–250.
21. Kumar AJ, *et al* (2000) Malignant Gliomas: MR Imaging Spectrum of Radiation Therapy and Chemotherapy-induced Necrosis of the Brain after Treatment. Radiology **217**: 377–384.

Received on March 25, 2011
Revision received on June 27, 2011
Accepted on July 14, 2011
J-STAGE Advance Publication Date: September 16, 2011